Phasor model of full scale converter wind turbine for small-signal stability analysis

Ghiga, Radu; Wu, Qiuwei; Nielsen, Arne Hejde

Published in:
The Journal of Engineering

Link to article, DOI:
10.1049/joe.2017.0476

Publication date:
2017

Document Version
Publisher's PDF, also known as Version of record

The 6th International Conference on Renewable Power Generation (RPG)

19–20 October 2017

Phasor model of full scale converter wind turbine for small-signal stability analysis

Radu Gihga, Qiuwei Wu, Arne Hejde Nielsen

Centre for Electric Power and Energy, Department of Electrical Engineering, Technical University of Denmark, Denmark
E-mail: qw@elektro.dtu.dk

Published in *The Journal of Engineering*; Received on 9th October 2017; Accepted on 1st November 2017

Abstract: The small-signal stability analysis of power system electromechanical oscillations is a well-established field in control and stability assessment of power systems. The impact of large wind farms on small-signal stability of power systems has been a topic of high interest in recent years. This study presents a phasor model of full scale converter wind turbines (WTs) implemented in MATLAB/SIMULINK for small-signal stability studies. The phasor method is typically used for dynamic studies of power systems consisting of large electric machines. It can also be applied to any linear system. This represents an advantage in small-signal stability studies, which are based on modal analysis of the linearised model and are usually complemented with dynamic simulations. The proposed model can represent a single WT or an aggregated wind power plant. The implemented model for small-signal stability analysis was tested in the Kundur's two area system. The results show that the proposed WT model is accurately linearised and its impact on power system oscillation is similar to that of previous research findings.

1 Introduction

The installed capacity of wind power and the size of each installation have been increasing rapidly, with the European offshore sector installation just over 3 GW of wind power only in 2015 [1]. The role and impact of large penetration of wind power can be significant in the operation and security of the power system [2, 3]. A topic of interest is the effect of large wind power plants (WPPs) on small-signal stability of power systems. The validity of the damping results depends on accurate representation of the WPP control systems [4–6].

In a full scale converter wind turbine (FSCWT), the generator dynamics are decoupled from the grid dynamics. Hence, the wind turbine (WT) generator cannot contribute to damping the system oscillations without additional control [7]. However, this type of configuration has the advantage of controlling both active and reactive power independently, and also allows independent impact assessment of these controls on power system oscillations.

The phasor simulation method in MATLAB/SIMULINK is typically used to study low frequency electromechanical oscillations of power systems consisting of a large number of generators and loads. An advantage of this method is that sinusoidal voltages and currents are replaced with phasors expressed in the complex or polar form. Since the electromagnetic transients are not of interest, the dynamic simulation time is reduced [8]. Another advantage is that the phasor simulation can be used with any linear system, and small-signal stability studies are based on eigenvalue analysis of the linearised power system. Finally, the eigenvalue analysis is usually complemented with dynamic simulations of the non-linear system which can be several tens of seconds long. Hence, short simulation times are desired.

The aim of this paper is to present a FSCWT model that can be used in dynamic simulations, and can be linearised by the tools available in SIMULINK, without the need to build a separate state-space representation of the model. Therefore, a phasor FSCWT model with a permanent magnet synchronous generator (PMSG) is implemented in MATLAB/SIMULINK. The model consists of detailed controls in order to catch the potential impact, which might have on power system oscillations. The eigenvalues of the system are first analysed with no wind power injected in the network, and then with increasing wind power penetration. To verify the accuracy of the linearised system, the linear and non-linear responses of the system are compared.

This paper is organised as follows. In Section 2, the WT concept is presented. Section 3 describes the controls implemented for this model. Section 4 shows the results and conclusions are drawn in Section 5.

2 WT concept

The concept of the FSCWT is shown in Fig. 1. The main parts are the WT rotor, PMSG, FSC, filter, and transformer. The FSC consists of a generator side and grid side that are connected by a DC-link circuit with a capacitor (C_{dc}). The generator three-phase AC voltage is converted into DC voltage (V_{dc}) by the generator side converter. The DC voltage is then inverted back into AC by the grid side converter which uses a phase-locked loop (PLL) to match the grid frequency and phase.

The control system of the FSCWT consists of three main controllers. The pitch controller regulates the angle of the blades (β) to prevent the rotor speed (ω_r) from exceeding its rated value. The generator side control adjusts the generator currents in order to control its active (P_{gen}) and reactive power (Q_{gen}) outputs. The grid side control maintains V_{dc} to its rated value, and controls the reactive power (Q_{grid}) output and the AC voltage at the terminal of the WT.

3 WT phasor model

The block diagram of the WT phasor model implemented in SIMULINK is shown in Fig. 2. The V_{abc}/V_{dq} block has a PLL implemented that computes the angle of the terminal voltage phasor and uses it to align the internal dq-reference. The WT is interfaced with the network through a controlled current source and connected to the grid at the point of connection (POC). The remaining blocks are described in the following subsections.

3.1 Aerodynamic model and pitch controller

The Aerodynamics block calculates the mechanical torque (T_m) as $T_m = P_m/\omega_r$. The mechanical power P_m converted from the wind

doi: 10.1049/joe.2017.0476

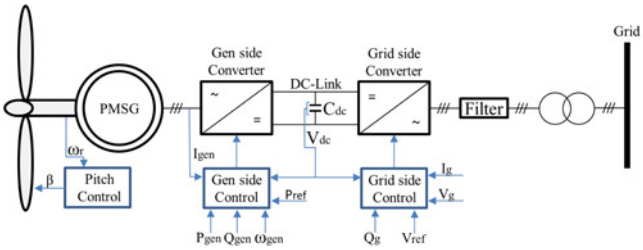

Fig. 1 *Wind turbine concept*

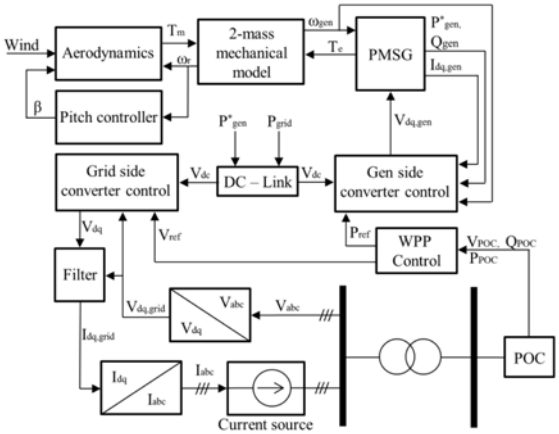

Fig. 2 *Block diagram of the phasor model*

speed is calculated inside this block as [9]

$$P_{\mathrm{m}} = 0.5\rho A v^3 C_{\mathrm{p}}(\lambda, \beta) \tag{1}$$

where ρ is the air density (kg/m^3), A is the rotor swept area (m^2), v is the wind speed (m/s), C_{p} is the power coefficient, and λ is the tip speed ratio (v_{t}/v), and v_{t} is the blade tip speed (m/s). The generic equation used to approximate C_{p} is given in [9].

Fig. 3 shows the pitch controller of the WT. The blade pitch angle (β) is calculated based on the error between the measured rotor speed and the reference value (ω_{ref} = 1.0 p.u.). The angle is kept at zero degree as long as the rotor speed does not exceed the reference value. An angle change rate limiter is implemented to model the blade rotation speed.

3.2 Mechanical model

The mechanical model is used to simulate the WT drive train which consists of the rotor hub with blades, rotor shaft, and generator rotor. In order to reflect the torsional shaft oscillations that can occur due to a sever network disturbance, a two-mass model should be implemented [10]. This model is also adequate when investigating the effect of wind gusts, or the change in the active power set-point [11].

Fig. 4 shows the mechanical model implemented in this paper, where H_{t} and H_{g} are the inertia constants of the rotor and generator,

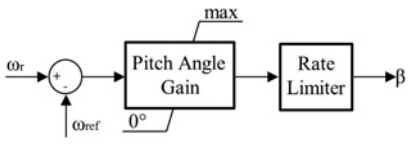

Fig. 3 *Pitch controller*

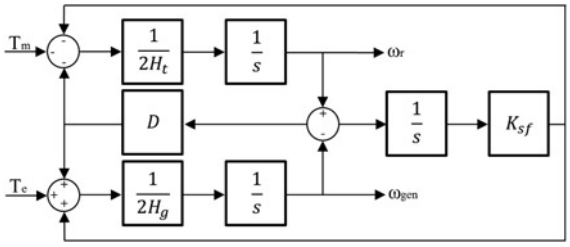

Fig. 4 *Mechanical model (2-mass model)*

respectively [12]. The damping coefficient is D, and the shaft stiffness is K_{sf}.

3.3 Converter control models

The block diagram of the generator side converter control is shown in Fig. 5. The reactive power reference (Q_{ref}) is set to zero and the converter controls the d-axis current ($I_{\mathrm{d,gen}}$) to achieve unity power factor at the generator terminals. The active power reference (P_{ref}) can be calculated based on a maximum power point tracking method [13], or it can be given by the WPP control as shown in Fig. 2. The generator side controller adjusts the q-axis current ($I_{\mathrm{q,gen}}$) in order to control the active power production (P_{gen}).

The grid side converter control shown in Fig. 6 keeps the DC-link voltage (V_{dc}) to its nominal value by controlling the d-axis grid current ($I_{\mathrm{d,grid}}$). The AC voltage and reactive power at the WT terminal are controlled by adjusting the q-axis current ($I_{\mathrm{q,\ grid}}$).

The reference voltage (V_{ref}) is calculated in the WPP control block and sent to the WT in order to keep the AC voltage at the terminal to its rated value. The block diagram in Fig. 6 is based on [14].

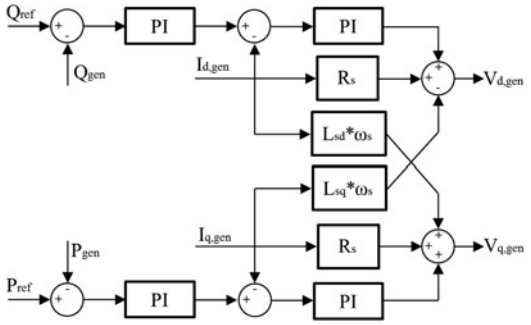

Fig. 5 *Generator side controller*

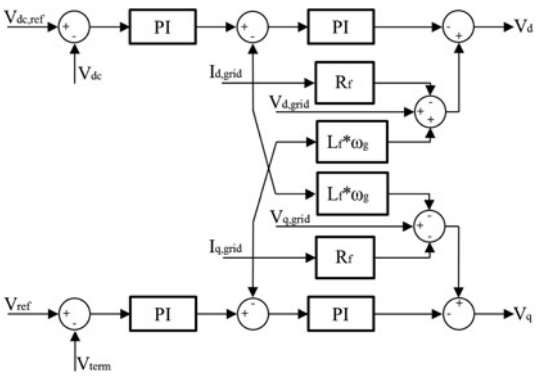

Fig. 6 *Grid side converter controller*

3.4 PMSG phasor model

The MATLAB/SIMULINK library documentation [8] provides the differential equations of the generator electrical model in the d–q rotor reference frame, where all the quantities in the rotor reference frame are referred to the stator as

$$\frac{\mathrm{d}}{\mathrm{d}t}I_{\mathrm{d,gen}} = \frac{V_{\mathrm{d,gen}}}{L_{\mathrm{sd}}} - \frac{R_{\mathrm{s}}}{L_{\mathrm{sd}}}I_{\mathrm{d,gen}} + \frac{L_{\mathrm{sq}}}{L_{\mathrm{sd}}}I_{\mathrm{q,gen}}\omega_{\mathrm{s}} \tag{2}$$

$$\frac{\mathrm{d}}{\mathrm{d}t}I_{\mathrm{q,gen}} = \frac{V_{\mathrm{q,gen}}}{L_{\mathrm{sq}}} - \frac{R_{\mathrm{s}}}{L_{\mathrm{sq}}}I_{\mathrm{q,gen}} - \frac{L_{\mathrm{sd}}}{L_{\mathrm{sq}}}I_{\mathrm{d,gen}}\omega_{\mathrm{s}} - \frac{\psi_{\mathrm{m}}\omega_{\mathrm{s}}}{L_{\mathrm{sq}}} \tag{3}$$

where $I_{\mathrm{d\,q,gen}}$ are the stator current components, $V_{\mathrm{d\,q,gen}}$ are the stator voltage components, ω_{s} is the stator electrical frequency, ψ_{m} is the flux of the permanent magnets, and $L_{\mathrm{s\,d,q}}$ are the d-axis and q-axis inductances. The block diagram of the generator electric phasor model implemented in SIMULINK is shown in Fig. 7.

3.5 DC-link model

The power generated by the PMSG is supplied to the grid side converter through the DC-link. The dynamics of the capacitor voltage (V_{dc}) can be expressed as [15]

$$\frac{\mathrm{d}V_{\mathrm{dc}}}{\mathrm{d}t} = \left(P_{\mathrm{gen}} - P_{\mathrm{grid}}\right)\frac{1}{V_{\mathrm{dc}}C_{\mathrm{dc}}} \tag{4}$$

The block diagram of the model is shown in Fig. 8.

3.6 Grid side RL filter phasor model

The WT is connected to the transformer through a three-phase RL filter. The single-phase equivalent circuit is shown in Fig. 9, and the model is described by the following differential equations [16]

$$V_{\mathrm{conv}} - V_{\mathrm{grid}} = L_{\mathrm{f}}\frac{\mathrm{d}I}{\mathrm{d}t} + R_{\mathrm{f}}I \tag{5}$$

where V_{conv} is the voltage at the converter side, and V_{grid} is the voltage at the grid side, and L_{f} and R_{f} are the filter inductance and resistance, respectively. The differential equations of the filter in the rotating d–q frame are as follows:

$$I_{\mathrm{d}} = \frac{\omega}{L_{\mathrm{f}}s}\left(V_{\mathrm{d}} - V_{\mathrm{d,grid}} - R_{\mathrm{f}}I_{\mathrm{d}} + L_{\mathrm{f}}I_{\mathrm{q}}\right) \tag{6}$$

$$I_{\mathrm{q}} = \frac{\omega}{L_{\mathrm{f}}s}\left(V_{\mathrm{q}} - V_{\mathrm{q,grid}} - R_{\mathrm{f}}I_{q} - L_{\mathrm{f}}I_{\mathrm{d}}\right) \tag{7}$$

where $\omega = 2\pi F_{\mathrm{now}}$, and V_{d}, V_{q} are the dq-components of V_{conv}. The filter block diagram is shown in Fig. 10.

3.7 WPP control (WPPC)

The WPPC in Fig. 2 measures the voltage (V_{POC}), active (P_{POC}) and reactive (Q_{POC}) powers at the POC. It sends voltage and active power references to the WPP. In this paper, the WPPC consists of an active power controller shown in Fig. 11, and a voltage controller shown in Fig. 12.

The active power control is a simplified version of the one in [11]. The power reference (P_{ref}) is decided as the minimum between the optimal power (P_{opt}) and a value (P_{set}) chosen by the transmission system operator or WPP owner. In this paper, the WPP is an aggregated model and P_{opt} is calculated based on the MPPT method from [13].

A similar voltage control has been used in [7]. It calculates a voltage reference (V_{ref}) based on the measured reactive power (Q_{POC}) and measured voltage (V_{POC}), and sends it to the WPP. Consequently, the WPP adjusts its output accordingly so the

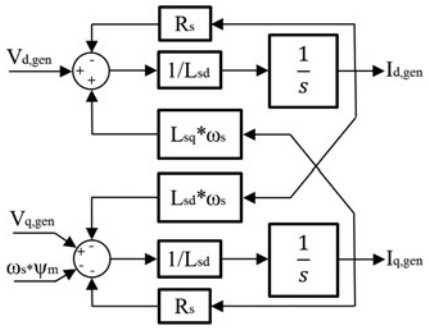

Fig. 7 *Block diagram of the generator model*

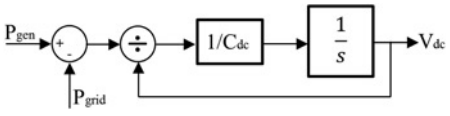

Fig. 8 *DC-link model*

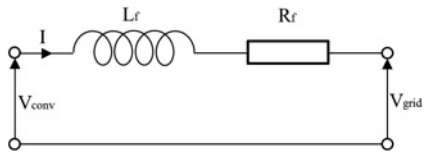

Fig. 9 *Single-phase RL-filter equivalent circuit*

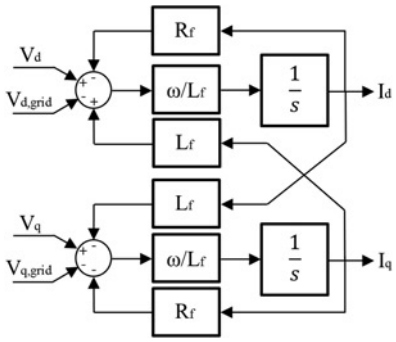

Fig. 10 *RL filter block diagram in d–q rotating frame*

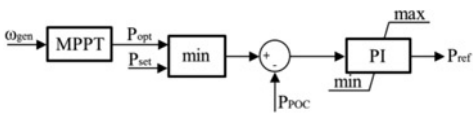

Fig. 11 *Wind park active power controller*

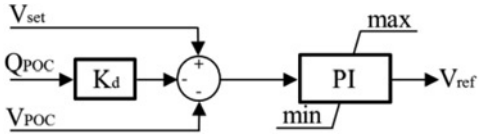

Fig. 12 *Wind park voltage controller*

Table 1 WPP collector system parameters

Collector parameters			Park transformer
R^*, Ω	X_L^*, Ω	B_C^*, μS	X_T, %
0.086	0.070	3219.7	12.2

voltage at the POC matches the reference voltage in the WPPC. The value of the droop gain K_d is 0.04 as given in [7].

3.8 Wind park collector system

The aggregated model of the WPP is connected to the grid through a collector system modelled as a T-equivalent. For a WPP of 180 MW, the collector system parameters are given in Table 1. Depending on the size of the WPP, the parameters are scaled using (8) and (9) so the voltage profile remains the same [7]

$$z_{\text{scale}} = \frac{S^*_{\text{base}}}{S_{\text{baseWP}}}; \quad R_{\text{col}} = z_{\text{scale}} R^* \tag{8}$$

$$X_L = z_{\text{scale}} X^*_L; \quad B_{\text{col}} = \frac{B^*_C}{z_{\text{scale}}} \tag{9}$$

4 Simulation results

The analysis is performed in MATLAB/SIULINK where the power system model is implemented using the SimPowerSystems [17]. The phasor WT model presented in the previous section is included in the power system network as an aggregated WPP, and the small-signal stability is assessed by linearising the model. The linearisation is performed using the Simulink control design toolbox [18], directly on the initialised power system model. The control design toolbox uses exact linearisation for every function in the model that has an analytical first derivative, and numerical perturbation is used for elements, such as look-up tables, that cannot be linearised analytically. This study is based on the Kundur's two area system shown in Fig. 13 to which the WPP is added. All generators are equipped with power system stabilisers (PSS) which are tuned as in [19].

4.1 Case study without wind power

The modal characteristics of the power system without wind power are analysed first. The model is linearised and its eigenvalues are computed. One inter-area mode and two local area modes are present in the system and their characteristics are given in Table 2. These values are very similar to the eigenvalues presented in [19] for the two area network, thus confirming these results are correct.

The modal analysis is complemented with time domain simulations of both the linear and non-linear systems in order to validate the linearisation of the model. The oscillations are excited by a step

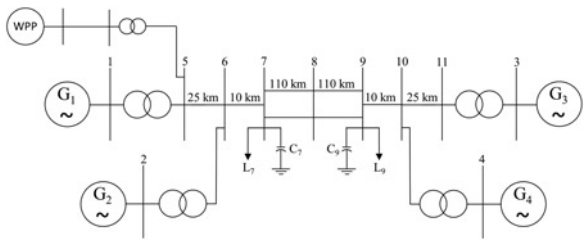

Fig. 13 *Kundur's two area system case study*

Table 2 Modal characteristics of the power system without wind penetration

Type of control	Eigenvalue/(frequency in Hz, damping ratio)		
	Inter-area mode	Area 1 local mode	Area 2 local mode
PSS	−0.689 ± j4 (f = 0.65, ζ = 0.17)	−2.56 ± j8.42 (f = 1.4, ζ = 0.291)	−2.49 ± j8.9 (f = 1.47, ζ = 0.269)

increase of 1% in the excitation voltage reference of G_1. The rotor speeds of generators G_1 and G_3 are shown in Fig. 14. The inter-area mode is clearly visible as the generators swing against each other. The linear and non-linear model responses overlap, validating the linearisation.

4.2 Case study with wind power

For this case, the aggregated phasor WPP model is included in the two area system at bus 5 as shown in Fig. 13. The wind power injected in the system is increased from 30 to 560 MW in five steps. The WPP is a scaled up 5 MW WT with the parameters of the generator and drive train given in Table 3.

It is known that the modal characteristics of the power system can be affected by a significant change in the dispatch of existing power units and the power flow [20]. In this study, the influence of the proposed WT model on the power system oscillations is of interest. Therefore, the system power flow is kept unchanged by lowering the power set-point of generator G_1 for each step increase in wind power. The dispatch of the other three generators remains constant, and so does the MVA rating of all generators.

The entire model is linearised and the modal characteristics of the system with wind power are shown in Table 4. The results confirm that the full-load converter WT model has a small effect on the

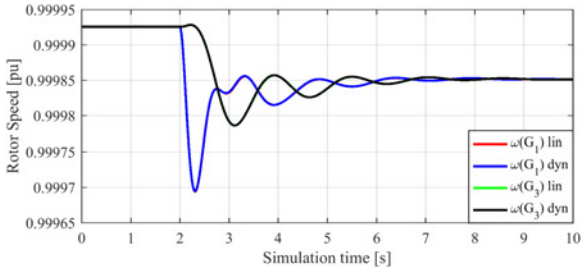

Fig. 14 *Rotor response of generators G_1 and G_3 with no wind power*

Table 3 Parameters for the wind turbine

Permanent magnet synchronous generator	
Parameter	Value
rated power (P_{nom})	5 MW
rated voltage (V_{nom})	0.69 kV
R_s	0.017 pu
L_{sd}	1.0 pu
L_{sq}	0.7 pu
Ψ_m	1.4 pu
drive train	
H_t	6.0 s
H_g	0.9 s
D	1.5
K_{sf}	296

Table 4 Modal characteristics of the power system with wind penetration

Wind power, MW	Eigenvalue/(frequency in Hz, damping ratio) with wind power		
	Inter-area mode	Area 1 local mode	Area 2 local mode
30	$-0.692 \pm j3.99$ ($f=0.64$, $\zeta=0.171$)	$-2.6 \pm j8.35$ ($f=1.39$, $\zeta=0.297$)	$-2.49 \pm j8.9$ ($f=1.47$, $\zeta=0.269$)
50	$-0.694 \pm j3.99$ ($f=0.64$, $\zeta=0.171$)	$-2.62 \pm j8.3$ ($f=1.39$, $\zeta=0.301$)	$-2.49 \pm j8.9$ ($f=1.47$, $\zeta=0.269$)
100	$-0.699 \pm j3.97$ ($f=0.64$, $\zeta=0.173$)	$-2.67 \pm j8.18$ ($f=1.37$, $\zeta=0.311$)	$-2.49 \pm j8.9$ ($f=1.47$, $\zeta=0.269$)
200	$-0.707 \pm j3.94$ ($f=0.63$, $\zeta=0.176$)	$-2.74 \pm j7.92$ ($f=1.33$, $\zeta=0.327$)	$-2.49 \pm j8.89$ ($f=1.47$, $\zeta=0.27$)
560	$-0.704 \pm j3.79$ ($f=0.61$, $\zeta=0.182$)	$-2.6 \pm j7.02$ ($f=1.19$, $\zeta=0.347$)	$-2.49 \pm j8.89$ ($f=1.47$, $\zeta=0.27$)

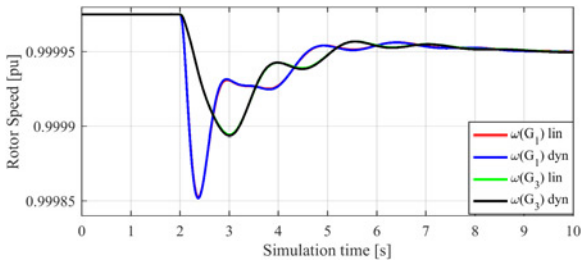

Fig. 15 *Rotor responses of generators G_1 and G_3 with 560 MW wind power*

inter-are mode which is in agreement with previous findings [7]. Fig. 15 shows the rotor speeds of generators G_1 and G_3 for the linear and non-linear models. The responses match and the inter-area oscillation is visible as the two generators swing against each other.

The step change in the excitation voltage causes the G_1 terminal voltage to change. This affects the voltage at bus 5 where the WT is connected. The WPP voltage control measures this change and acts on it. The responses of the voltage and reactive power change are shown in Figs. 16 and 17, respectively. The responses of the linear and non-linear models overlap, confirming that the model has been linearised correctly.

As the full-load converter decouples the WT generator and drive-train dynamics from the grid dynamics, the active power output of the WT is not affected by the change in voltage. This is shown in Fig. 18 where the active power of both linear and non-linear models match, and remain unchanged during the disturbance.

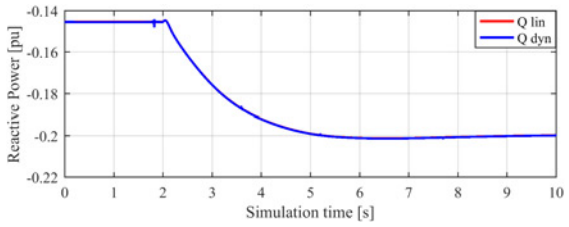

Fig. 16 *Reactive power at WPP PCC*

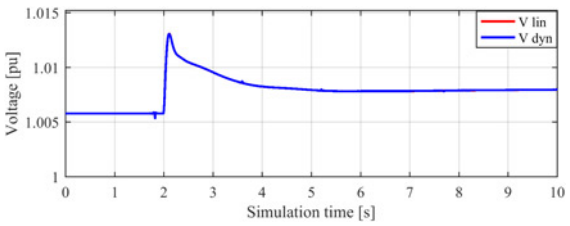

Fig. 17 *Voltage at WPP PCC*

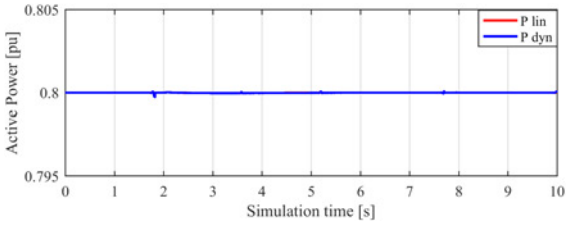

Fig. 18 *Active power at WPP PCC*

Table 5 Normalised rotor participation factors

State variable	Participation factors for inter-area mode
δ (G_1)	0.32
δ (G_2)	0.15
δ (G_3)	1
δ (G_4)	0.87
δ_r (WPP)	$<10^{-2}$

The degree of interaction of the WPP and generators in the inter-area oscillation is evaluated with the aid of the normalised participation factors shown in Table 5. Generator G_3 has the highest participation in the inter-area mode, while the WT has a negligible effect on this mode shape. A similar conclusion is drawn in [7].

5 Conclusion

In this paper, a phasor model of a FSCWT for small-signal stability assessment is implemented in MATLAB/SIMULINK. The Simulink control design toolbox is used to linearise the entire initialised model and the linearisation result is validated by comparing the step responses of the linear and non-linear systems with dynamic simulations. The results show that the responses match for small disturbances (1% step in generator excitation voltage reference). Hence, the phasor model is linearised accurately.

The modal characteristics of the test system are analysed with and without wind power, and the results match previous research findings. The participation factors show that the FSCWT does not have a significant impact on the inter-area mode, which confirms the results from previous research. Therefore, the proposed model can be used either as a single WT or as an aggregated model to perform small-signal stability studies of power systems with large wind penetration.

6 References

[1] Global wind energy Report 2015. Available at http://www.gwec.net/publications/global-wind-report-2/, accessed April 2016

[2] Akhmatov V., Knudsen H., Nielsen A.H., *ET AL.*: 'Modelling and transient stability of large wind farms', *Int. J. Electr. Power Energy Syst.*, 2003, **25**, pp. 123–144

[3] Ledesma P., Usaola J., Rodriguez J.: 'Transient stability of a fixed speed wind farm', *Renew. Energy*, 2003, **28**, (9), pp. 1341–1355

doi: 10.1049/joe.2017.0476

[4] Rostamkolai N., Piwko R.J., Larsen E.V., *ET AL.*: 'Subsynchronous interactions with static VAR compensators-concepts and practical implications', *IEEE Trans. Power Syst.*, 1990, **5**, pp. 1324–1332
[5] Tang J.: 'Reader's guide to subsynchronous resonance', *IEEE Trans. Power Syst.*, 1992, **7**, pp. 150–157
[6] Tsourakis G., Nomikos B.M., Vournas C.D.: 'Effect of wind parks with doubly fed asynchronous generators on small-signal stability', *Electr. Power Syst. Res.*, 2009, **79**, pp. 190–200
[7] Knuppel T., Nielsen J.N., Jensen K.H., *ET AL.*: 'Small-signal stability of wind power system with full-load converter interfaced wind turbines', *IET Renew. Power Gener.*, 2012, **6**, pp. 79–91
[8] MATLAB documentation center. Available at https://wwxw.mathworks.com/help/
[9] Heier S.: 'Grid integration of wind energy conversion systems' (John Wiley & Sons, New York, 1998)
[10] Anderson P.M.: 'Subsynchronous resonance in power system' (IEEE Press, New York, 1994)
[11] Hansen A.D., Margaris I.D.: 'Type IV wind turbine model DTU wind energy', 2014. Available at http://orbit.dtu.dk/en/publications/type-iv-wind-turbine-model(99b55843-deb3-49b9-b564-e664bc25fa99).html
[12] Miller N.W., Pric W.W., Samches-Gasca J.J.: 'Dynamic modeling of GE 1.5 and 3.6 wind turbine-generators' (GE-Power System Energy Consulting, 2003). Available at https://pdfs.semanticscholar.org/4be9/52ff4ee3203db24ed461f8064abb00b8fa4e.pdf
[13] Muyeen S.M., Tamura J., Murata T.: 'Stability augmentation of a grid connected wind farm, green energy and technology' (Springer-Verlag, Berlin, 2009)
[14] Blasko V., Kaura V.: 'A new mathematical model and control of a three-phase AC-DC voltage source converter', *IEEE Trans. Power Electron.*, 1997, **12**, pp. 116–123
[15] Fernandez L.M., Garcia C.A., Jurado F.: 'Operating capability as a PQ/PV node of a direct-drive wind turbine based on a permanent magnet synchronous generator', *J. Renew. Energy*, 2010, **35**, pp. 1308–1318
[16] Santiprapan P., Areerak K.-L., Areerak K.-N.: 'Mathematical model and control strategy on DQ frame for shunt active power filters', *Int. J. Electr. Comput. Energ. Electron. Commun. Eng.*, 2011, **5**, (12), pp. 1664–1671
[17] MATLAB documentation center, SimPowerSystems™ 6.6 – User's Guide, 2016
[18] MATLAB documentation center, Simulink Control Design™ 4.4 – User's Guide, 2016
[19] Kundur P.: 'Power system stability and control' (McGraw-Hill, New York, NY, USA, 1994)
[20] Wilson D., Bialek J., Lubosny Z.: 'Banishing blackouts [power system oscillations stability]', *Power Eng.*, 2006, **20**, pp. 38–41